BioOne COMPLETE

Heterochromatin Domain Number Correlates with X-Ray and Carbon-Ion Radiation Resistance in Cancer Cells

Authors: Sato, Katsutoshi, Imai, Takashi, Okayasu, Ryuichi, and Shimokawa, Takashi

Source: Radiation Research, 182(4) : 408-419

Published By: Radiation Research Society

URL: https://doi.org/10.1667/RR13492.1

BioOne Complete (complete.BioOne.org) is a full-text database of 200 subscribed and open-access titles in the biological, ecological, and environmental sciences published by nonprofit societies, associations, museums, institutions, and presses.

Your use of this PDF, the BioOne Complete website, and all posted and associated content indicates your acceptance of BioOne's Terms of Use, available at www.bioone.org/terms-of-use.

Usage of BioOne Complete content is strictly limited to personal, educational, and non - commercial use. Commercial inquiries or rights and permissions requests should be directed to the individual publisher as copyright holder.

BioOne sees sustainable scholarly publishing as an inherently collaborative enterprise connecting authors, nonprofit publishers, academic institutions, research libraries, and research funders in the common goal of maximizing access to critical research.

Downloaded From: https://bioone.org/journals/Radiation-Research on 29 Mar 2024
Terms of Use: https://bioone.org/terms-of-use

RADIATION RESEARCH **182**, 408–419 (2014)
0033-7587/14 $15.00
©2014 by Radiation Research Society.
All rights of reproduction in any form reserved.
DOI: 10.1667/RR13492.1

Heterochromatin Domain Number Correlates with X-Ray and Carbon-Ion Radiation Resistance in Cancer Cells

Katsutoshi Sato,[a,b] Takashi Imai,[b] Ryuichi Okayasu[c] and Takashi Shimokawa[a,1]

[a] *Cancer Metastasis Research Team;* [b] *Advanced Radiation Biology Research Program, Research Center for Charged Particle Therapy; and* [c] *International Open Laboratory, National Institute of Radiological Sciences, Chiba, Japan*

Sato, K., Imai, T., Okayasu, R. and Shimokawa, T. Heterochromatin Domain Number Correlates with X-Ray and Carbon-Ion Radiation Resistance in Cancer Cells. *Radiat. Res*. 182, 408–419 (2014).

Although it is known that cancer cells can develop radiation resistance after repeated exposures to X rays, the underlying mechanisms and characteristics of this radiation-induced resistance of cancer cells are not well understood. Additionally, it is not known whether cells that develop X-ray resistance also would develop resistance to other types of radiation such as heavy-ions including carbon ions (C-ion). In this study, we established X-ray resistant cancer cell lines by delivering repeated exposures to X rays, and then assessed whether the cells were resistant to carbon ions. The mouse squamous cell carcinoma cell line, NR-S1, was X irradiated six times with 10 Gy, and the X-ray resistant cancer cells named X60 and ten subclones were established. Significant X-ray resistance was induced in four of the subclones (X60, X60-H2, X60-A3 and X60-B12). The X60 cells and all of the subclones were resistant to carbon ions. The correlation analysis between radioresistance and morphological characteristics of these cells showed that X-ray ($R = 0.74$) and C-ion ($R = 0.79$) resistance correlated strongly with the number of heterochromatin domains. Moreover, the numbers of γ-H2AX foci remaining in irradiated X60 cells and radioresistant subclones X60-A3 and X60-H2 were lower than in the NR-S1 cells after X-ray or C-ion irradiation, indicating that X60 cells and the radioresistant subclones rapidly repaired the DNA double-strand breaks compared with NR-S1 cells. Our findings suggest that the underlying causal mechanisms of X-ray and C-ion radiation resistance may overlap, and that an increase in heterochromatin domain number may be an indicator of X-ray and C-ion resistance. © 2014 by Radiation Research Society

Editor's note. The online version of this article (DOI: 10.1667/RR13492.1) contains supplementary information that is available to all authorized users.

[1] Address for correspondence: Cancer Metastasis Research Team, Advanced Radiation Biology Research Program, Research Center for Charged Particle Therapy, National Institute of Radiological Sciences, 4-9-1, Anagawa, Inage-ku, Chiba, 263-8555, Japan; e-mail: takshi@nirs.go.jp.

INTRODUCTION

The recent development of techniques used in radiotherapy such as hypofractionated radiation therapy now allow us to curatively treat early stages of some cancer (*1, 2*). In particular, the therapeutic outcome of early stage lung cancer treated with hypofractionated radiation therapy was shown to be comparable to that of surgical resection. However, in some cases, tumors do reoccur even after high dose radiotherapy (*2*). Tumor recurrence after a course of radiation treatments can be extremely difficult to control, because retreatment with radiation therapy is limited by the tolerance dose to normal tissues surrounding the tumor that has previously undergone treatment, and the treated tumor has possibly developed an X-ray-induced resistance to radiation. However, it has recently been shown that heavy-ion radiations, such as carbon ions (C-ion), can be precisely delivered for the retreatment of recurrent tumors (*3*). It is known that the relative biological effectiveness (RBE) of carbon ions can be greater than 2 because the linear-energy transfer (LET) of carbon ions is significantly higher than the LET for X rays, although the actual RBE values are dependent on both changes in the LET (*4*) and the hypoxic fraction of irradiated samples (*5, 6*). In addition to a high RBE, the very precise physical dose distribution of heavy-ion beams such as carbon can be very beneficial in cancer treatment (*7*). The LET of carbon ions reaches its maximum at the back end of the beam track, which is termed the Bragg peak, while LET of the beam entry region is relatively low. This means that carbon-ion therapy is able to deliver a significantly higher dose into the tumor while sparing the surrounding normal tissue and skin. Therefore, carbon-ion therapy can be more effective for X-ray resistant cancers such as melanoma and osteosarcoma (*8, 9*). Retreatment with carbon ions (*3*) is now being considered as a very useful strategy for the control of recurrent X-ray resistant tumors.

In recurrent tumors that have been previously treated with X ray, it is possible that the characteristics of the tumor such as sensitivity to X rays have changed during radiation treatment. Therefore, to successfully treat recurrent tumors with carbon ions, it is necessary to evaluate the biological effectiveness on X-ray resistant cancer cells derived from

Downloaded From: https://bioone.org/journals/Radiation-Research on 29 Mar 2024
Terms of Use: https://bioone.org/terms-of-use

irradiated recurrent tumors. Although X-ray-induced radiation resistance in various cancer cells has been reported in resistant tumors (*10–14*), to our knowledge investigations have never been done to determine whether radiation resistant cancer cells produced by repeated exposure to X rays are also resistant to carbon ions. In addition, the cellular and molecular mechanisms induced in X-ray and C-ion resistant cancer cells compared to their parental cancer cells have not been quantitatively assessed. If there is a correlation between radioresistance and a cellular or molecular end point, it might be possible to reveal the mechanisms of X-ray and C-ion induced resistance in cancer cells.

In this study, we investigated whether X-ray resistant cancer cells are also resistant to carbon ions and identified morphological end points that correlated with X-ray and C-ion resistance by establishing X-ray resistant cancer cells through repeated exposure to X rays using mouse cancer cell lines. We found that the repeated exposure to X rays induced not only X-ray resistance but also C-ion resistance in some subclones. Our findings indicate that there are some common damage-response pathways after X-ray and C-ion exposure. Moreover, we found that the heterochromatin domain number strongly correlates with X-ray resistance in established radioresistant cancer cells.

MATERIALS AND METHODS

Cell Lines

The cell lines used for this study were the mouse squamous cell carcinoma cell line NR-S1 (kindly provided by Dr. Koichi Ando, Medicine and Biology Division, Gunma University Heavy Ion Medical Center), and the radioresistant cell line X60 and its subclones (X60-A3, X60-A9, X60-B11, X60-B12, X60-C3, X60-D4, X60-D9, X60-H2, X60-2 and X60-4). The NR-S1 cells originated from squamous cell carcinoma that arose from buccal mucosa (*15*). The X60 cells were established by means of repeated X ray irradiation of the NR-S1 cells as described in the *Establishment of Radioresistance Cancer Cells* section. The radioresistant sublines were randomly selected from the X60 cells. All cells were maintained in Dulbecco's modified Eagle medium (Nissui Pharmaceutical Co. Ltd., Tokyo, Japan) containing 10% fetal bovine serum (Thermo Fisher Scientific Inc., Waltham, MA), 2 m*M* L-glutamine (Gibco®, Carlsbad, CA) and 0.1% penicillin/streptomycin (Gibco).

X-Ray and Carbon-Ion Exposure

The TITAN-320 (Shimadzu, Kyoto, Japan) was used for X-ray irradiation. The tube voltage, current, distance from X-ray focus to incident surface and the dose rate were 200 kV at peak, 20 mA, 60 cm and 1 Gy/min, respectively.

Carbon-ion irradiation was performed at the Heavy Ion Medical Accelerator in Chiba (HIMAC) at the National Institute of Radiological Sciences, Japan. The carbon-ion energy and dose rate were 290 MeV/nucleon and 5 Gy/min, respectively. For the carbon-ion irradiation, a 6 cm spread out Bragg peak (SOBP) in depth was adopted and the cells were irradiated at the center of the SOBP (*16*). The dose averaged LET at the center of the SOBP is 50 KeV/μm (*4*). X-ray and C-ion irradiations were performed at room temperature.

Establishment of Radioresistant Cancer Cells

NR-S1 cells were irradiated with 10 Gy of X rays once every two weeks. The cells were exposed to X rays six times for a total dose of 60 Gy, after which they were identified as X60 cells. After the last exposure, the cells were cultured under normal conditions for four weeks. Ten sublines were then cloned from the X60 cells and the cellular character of each cell line was assessed (Supplementary Fig. S1; http://dx.doi.org/10.1667/RR13492.1.S1).

Colony Formation Assay

Immediately after X-ray or C-ion irradiation, the cells were washed with phosphate buffered saline (PBS) (Nissui Pharmaceutical Co. Ltd.), harvested with Trypsin-EDTA (Gibco) and seeded onto cell culture dishes. Eight days after plating for colony formation, the cells were fixed and stained with 0.1% w/v methylene blue (Sigma-Aldrich LLC, St. Louis, MO) containing 30% v/v methanol (Wako Pure Chemical Industries Ltd., Osaka, Japan). Colonies containing more than 50 cells were counted as cells that survived. The survival fractions were plotted versus dose and fitted to a linear-quadratic model with a nonlinear least square algorithm.

Morphological Analysis

The cells were washed with PBS, fixed with 10% buffered formalin (Wako Pure Chemical Industries Ltd.) for 20 min and permeabilized with 0.1% Triton X-100 (Sigma-Aldrich). The cells were then stained with hematoxylin (Merck, Darmstadt, Germany) and eosin (Sakura Finetek Co. Ltd., Japan, Tokyo, Japan). The microscopic images of the cells were produced using an inverted microscope (BX51, Olympus Corp. Tokyo, Japan) with 200× magnification. The cellular size and shape were analyzed with ImageJ software (version 1.46n, National Institutes of Health, Bethesda, MD). Based on the elongation index, which was calculated by dividing the cell length by its width, the cells were classified into the following three groups: 1. rounded; 2. elongated and 3. spindle shapes, with elongation index of less than 2, 2 or more, but less than 3, and 3 or more, respectively. At least 100 cells were counted.

Measurement of Heterochromatin Domain Number

The cells were washed with PBS and fixed with ice cold 99.5% ethanol (Wako Pure Chemical Industries Ltd.) for 5 min. The cells were then washed again with PBS^- and the nuclei were stained with 10 μ*M* of Hoechst 33342 (Sigma-Aldrich). The microscopic image of the nucleus was obtained at 600× magnification with a fluorescent microscope (IX70, Olympus Corp.). The heterochromatin domain number was quantified with ImageJ software. At least 100 cells were counted.

Analysis of DNA Contents and Cell Cycle Distribution

The cells were washed with PBS, harvested with Trypsin-EDTA (Gibco) and fixed with ice cold 95% ethanol. The fixed cells were washed three times with PBS, then treated with 0.25 mg/ml of RNase A solution (Qiagen, Valencia, CA) at 37°C for 30 min and stained with 50 μg/ml of propidium iodide (Sigma-Aldrich) for 30 min on ice. The fluorescence intensity was measured by FACSCaliber™ (Becton Dickinson, San Jose, CA). DNA contents and percentages of cell cycle distribution were analyzed by FlowJo software (version 8.2, Tree Star Inc., Ashland, OR).

Measurement of Doubling Time

WST-8 solution (Cell Counting Kit-8, Dojindo Molecular Technologies Inc., Kumamoto, Japan) was used to measure cell proliferation. The cells were washed with PBS, harvested with

Downloaded From: https://bioone.org/journals/Radiation-Research on 29 Mar 2024
Terms of Use: https://bioone.org/terms-of-use

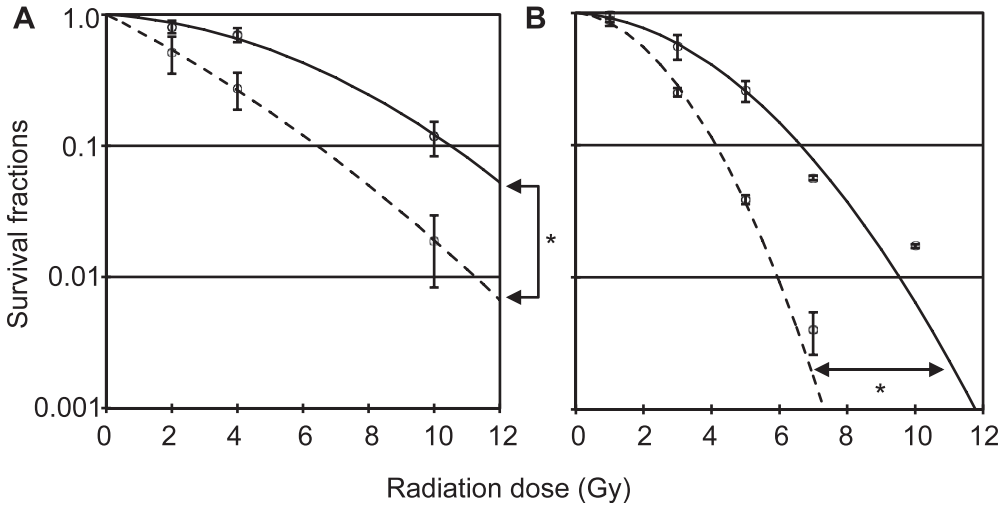


FIG. 1. Survival curves of NR-S1 (dashed line) and X60 (solid line) cell indicates the survival fractions after X-ray (panel A) and C-ion (panel B) irradiation. The values and the error bars indicate the mean and standard deviation, respectively, of 3–5 independent experiments with 3 replicates per experiment. Asterisks represent a significant difference of $P < 0.05$ tested with ANOVA.

Trypsin-EDTA (Gibco) and 500 cells were seeded into 96 well plates. On days 0, 1 and 3 after the cells had been seeded, 10 μl of WST-8 solution was added to each well and the cells were then incubated for 2 h at 37°C in a 5% CO_2 incubator. Optical density was measured by absorption photometer (ARVO™ X3, PerkinElmer Japan Co. Ltd.). The doubling time for each cell was calculated by comparing optical density at days 1 and 3.

Immunofluorescence Staining

The cells were washed three times with ice cold PBS, fixed with 10% buffered formalin for 20 min, then washed three times with 0.1 % Triton X-100 and blocked with 10% bovine serum albumin (Sigma-Aldrich) for 30 min. After blocking, the cells were incubated with anti-γ-H2AX antibody (clone JBW301, Upstate Biotechnology Inc., Lake Placid, NY) overnight at 4°C, then rinsed three times with PBS and incubated with DyLight 488 conjugated donkey anti-mouse IgG antibody (Jackson ImmunoResearch Laboratories Inc., West Grove, PA) for 1 h at room temperature. The nucleus was counterstained with 10 μ*M* of Hoechst 33342 (Sigma-Aldrich).

Statistical Analysis

The *t* test, two-way ANOVA and Pearson product-moment correlation coefficient were used to test for statistically significant differences in the mean values between the two groups, the differences in survival curve parameters, and the correlation coefficients, respectively. A *P* value of less than 0.05 was considered statistically significant for all analyses. All experiments were performed at least three times.

RESULTS

X-Ray and Carbon-Ion Sensitivity after Repeated Exposure to Radiation

The X60 cells were significantly more resistant to X radiation than the parental NR-S1 cells. When the cells were irradiated with 10 Gy X rays, the survival fractions of the X60 cells were 3.8-fold higher than that of the NR-S1 cells (Fig. 1A). In addition, the D10, the X-ray dose required to decrease the survival fraction to 10% or 0.1, was 10.5 Gy and 6.4 Gy in X60 and NR-S1 cells, respectively, meaning that X60 cells were 1.6-fold more resistant to X radiation compared with NR-S1 cells (Fig. 1A).

The X60 cells were also resistant to carbon ions. Cell survival of X60 cells after 5 Gy of carbon ions was increased 9.8-fold compared with that of NR-S1 cells (Fig. 1B). The D10 value of X60 and NR-S1 cells for carbon-ion irradiation was 6.4 and 3.9 Gy, respectively, and indicated that the X60 cells were 1.7-fold more resistant to carbon ions than NR-S1 cells (Fig. 1B).

The X60 cells are likely to contain many subpopulations with different radiosensitivities and cellular morphologies, since DNA damage was repeatedly induced in them by repeated X ray exposure. Therefore, we randomly established 10 subclones from the X60 cells and measured the X-ray and carbon-ion sensitivity of each clone by colony formation assay. Interestingly, X-ray and C-ion sensitivities for each subclone varied widely (Fig. 2). The significant X-ray resistant subclones were X60-H2, X60-A3 and X60-B12 cells when compared with the NR-S1 cells. On the other hand, X-ray sensitivities of X60-2, X60-C3, X60-D4, X60-D9, X60-A9 and X60-4 subclones were similar or slightly more resistant when compared with the NR-S1 cells. All subclones retained carbon-ion resistance compared with the NR-S1 cells, although the tendency was similar to their X-ray sensitivity. These results indicated that repeated exposure to X rays alters the radiosensitivity of the cells resulting in heterogeneous populations with significantly radioresistant cancer cells also being present as a part of this heterogeneous cell population. Moreover, the data suggest that the underlying mechanisms of X-ray resistance might overlap, partially, with that of carbon-ion radiation resistance.

Downloaded From: https://bioone.org/journals/Radiation-Research on 29 Mar 2024
Terms of Use: https://bioone.org/terms-of-use

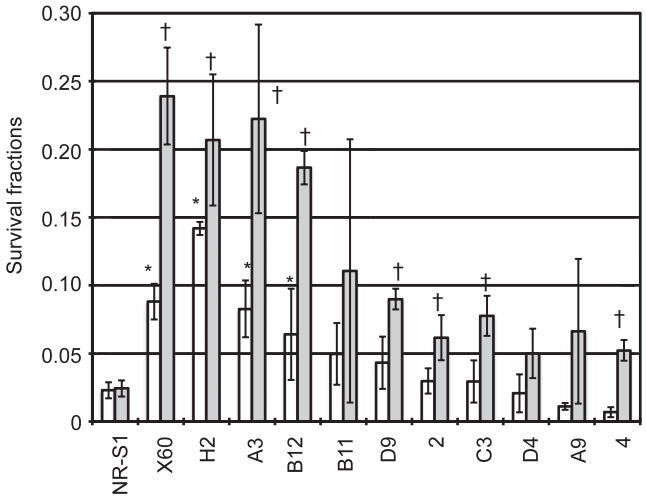


FIG. 2. The X-ray and carbon-ion sensitivity of NR-S1, X60 and each clone isolated from X60 cells. X60-H2, X60-A3, X60-B12, X60-B11, X60-D9, X60-2, X60-C3, X60-D4, X60-A9 and X60-4 cells are abbreviated to H2, A3, B12, B11, D9, 2, C3, D4, A9 and 4, respectively. These cells were irradiated with 10 Gy of X rays or with 5 Gy of carbon ions. White and gray boxes show the survival fractions after X-rays and C-ion irradiation, respectively. The values and error bars indicate the mean values and standard deviation, respectively, from 3 independent experiments with 3 replicates per experiment. Asterisks and daggers represent a significant difference of $P < 0.05$ using the t test.

Changes in Cellular Characteristics in Radioresistant Cells

After repetitive exposure to X rays, we found morphological alterations in the surviving cells. After the last irradiation, morphological features of the X60 cells were clearly altered from the parental NR-S1 cells. The cellular shapes of the X60 cells became spindle-like, the cell size became larger and the number of heterochromatin domains was clearly increased when compared with the NR-S1 cells (Fig. 3, Supplementary Fig. S2; http://dx.doi.org/10.1667/RR13492.1.S1). Additionally, each of the subcloned cells had different cellular shapes. We therefore measured the cellular size, shape and heterochromatin domain number for all cell lines and subclones. We counted the Hoechst 33342 intense foci as heterochromatin domains because we found that the Hoechst 33342 intense-foci colocalized well with HP1β (Supplementary Figs. S2 and S3; http://dx.doi.org/10.1667/RR13492.1.S1), which is a known marker of constitutive heterochromatin.

In X60 cells and most of the subclones, cellular size was significantly enlarged. However, these values showed wide variations and therefore are probably not associated with X-ray and carbon-ion resistance (Fig. 4A). However, the cellular shapes of many subclones were significantly elongated compared with NR-S1 cells (Fig. 4B). The results of stratifying the elongation index are indicated in Fig. 4C. In

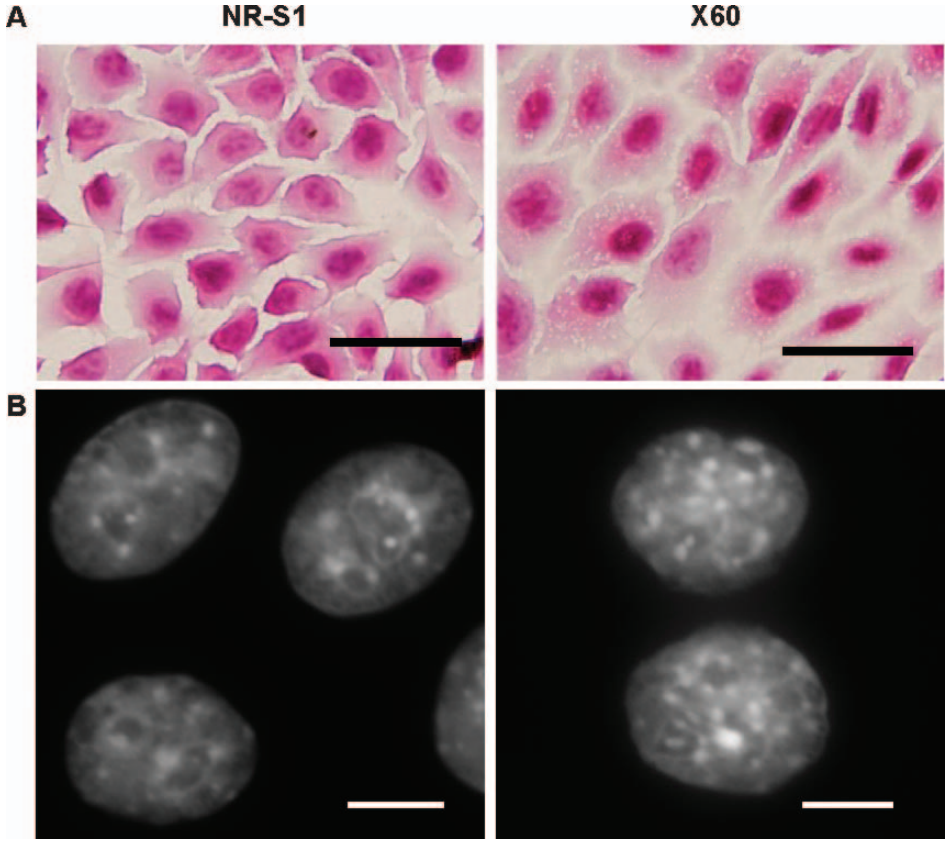


FIG. 3. Morphological difference between NR-S1 and X60 cells. Panel A shows the hematoxylin and eosin staining of the cultured cells. Panel B shows the nucleus that is stained with Hoechst 33342. The black and white scale bars indicate 50 μm and 10 μm, respectively.

Downloaded From: https://bioone.org/journals/Radiation-Research on 29 Mar 2024
Terms of Use: https://bioone.org/terms-of-use

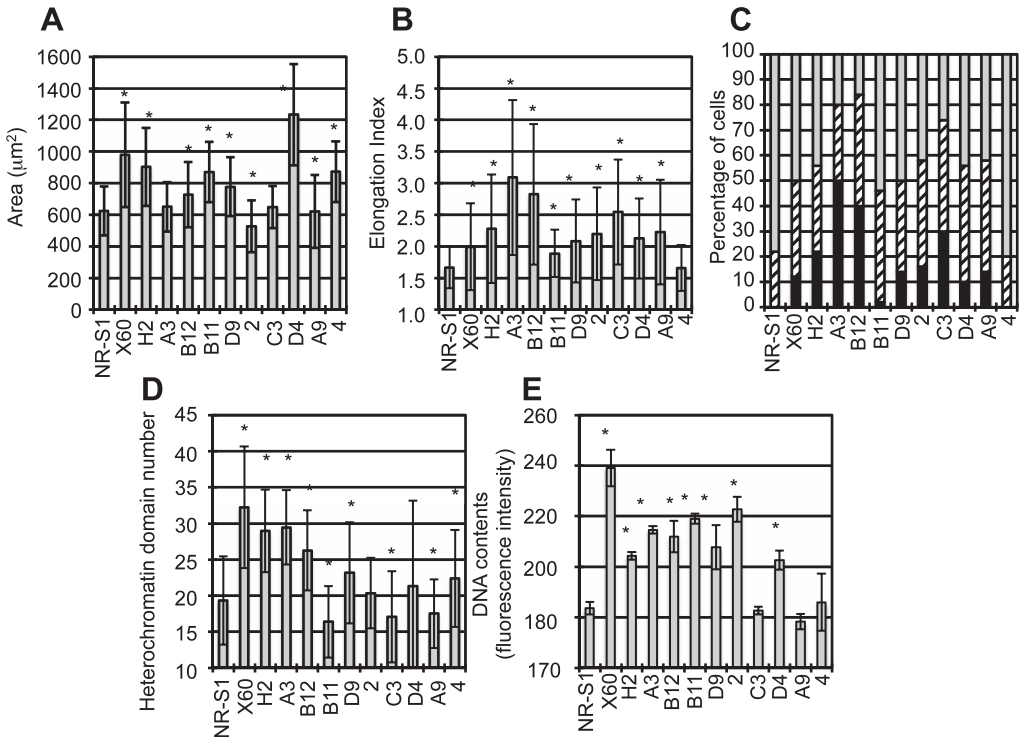


FIG. 4. Morphological difference between NR-S1, X60 cells and subclones. Panels A–E show the cellular size (panel A), shape (panel B), percentages of the stratified elongation index in counted cells (panel C), heterochromatin domain number (panel D), and DNA contents in G_1 phase (panel E) of NR-S1, X60 and each subclone. The values and error bars indicate the mean value and standard deviation, respectively. The DNA contents were acquired by 3 independent experiments. For the stratified elongation index, the rounded, elongated and spindle cells are shown as the gray, slashed and black boxes, respectively. The asterisk shows a significant difference of $P < 0.05$ using the t test.

the X60 cells and many of the subclones (excluding X60-B11 and X60-4 cells), the percentages of spindle and elongated cells were increased compared with the NR-S1 cells. The X60-B11 cells consisted of a few spindle cells, but contained many elongated cells. The distribution of the elongation index in X60-4 cells was approximately the same as for the NR-S1 cells. Interestingly, the heterochromatin domain number was significantly different between the radioresistant cells and nonradioresistant cells. In particular, the number of heterochromatin domains in the radioresistant subclone X60-H2, X60-A3 and X60-B12 cells were 1.5-, 1.5- and 1.4-fold higher, respectively, compared with that in the NR-S1 cells. Conversely, the heterochromatin domain number in other subclones was similar or lower when compared with that in NR-S1 cells.

Additionally, we assessed the DNA contents for all the clones using flow cytometer because the difference in heterochromatin domain number could imply changes in DNA content. The DNA content in most of the subclones, including the radioresistant subclone X60-H2, X60-A3 and X60-B12 cells, were significantly increased when compared with those of the NR-S1 cells although the incremental value was not high. Conversely, the DNA contents in X-ray sensitive subclone X60-C3, X60-A9 and X60-4 cells were similar to those in the NR-S1 cells (Fig. 4E).

We next investigated the basic cellular properties such as plating efficiency, doubling time and cell cycle distribution in normal culture conditions. The plating efficiencies of X60 cells and the majority of selected subclones significantly increased compared with the NR-S1 cells (Fig. 5A). In particular, the radioresistant X60, X60-H2, X60-A3 and X60-B12 cells showed 1.5-, 1.4-, 1.6- and 1.8-fold increase, respectively, in plating efficiency compared with NR-S1 cells. Conversely, the value in X60-A9 cells was significantly lower than that in NR-S1 cells. However, these plating efficiencies do not likely correlate with the radioresistance because the plating efficiencies fluctuated between cell lines. Analysis of the doubling time of each of the cell lines showed in general they were statistically the same as that of NR-S1 cells (Fig. 5B). However, the doubling time of X60-D4 cells was found to be significantly extended 1.5-fold compared with that of NR-S1 cells. Since cell cycle distribution is closely associated with cellular radiosensitivity, we next evaluated the cell cycle distribution in each cell line. The percentage of each phase was approximately the same in each cell (Fig. 5C–E), indicating no evidence for any association with the radioresistance of the cells. However, statistically significant differences were detected in X60-A3, X60-C3 and X60-D4 cells. In NR-S1 cells, the percentages of G_1, S and G_2/M phase were 38.5%, 42.9% and 27.2%, respectively. In

Downloaded From: https://bioone.org/journals/Radiation-Research on 29 Mar 2024
Terms of Use: https://bioone.org/terms-of-use

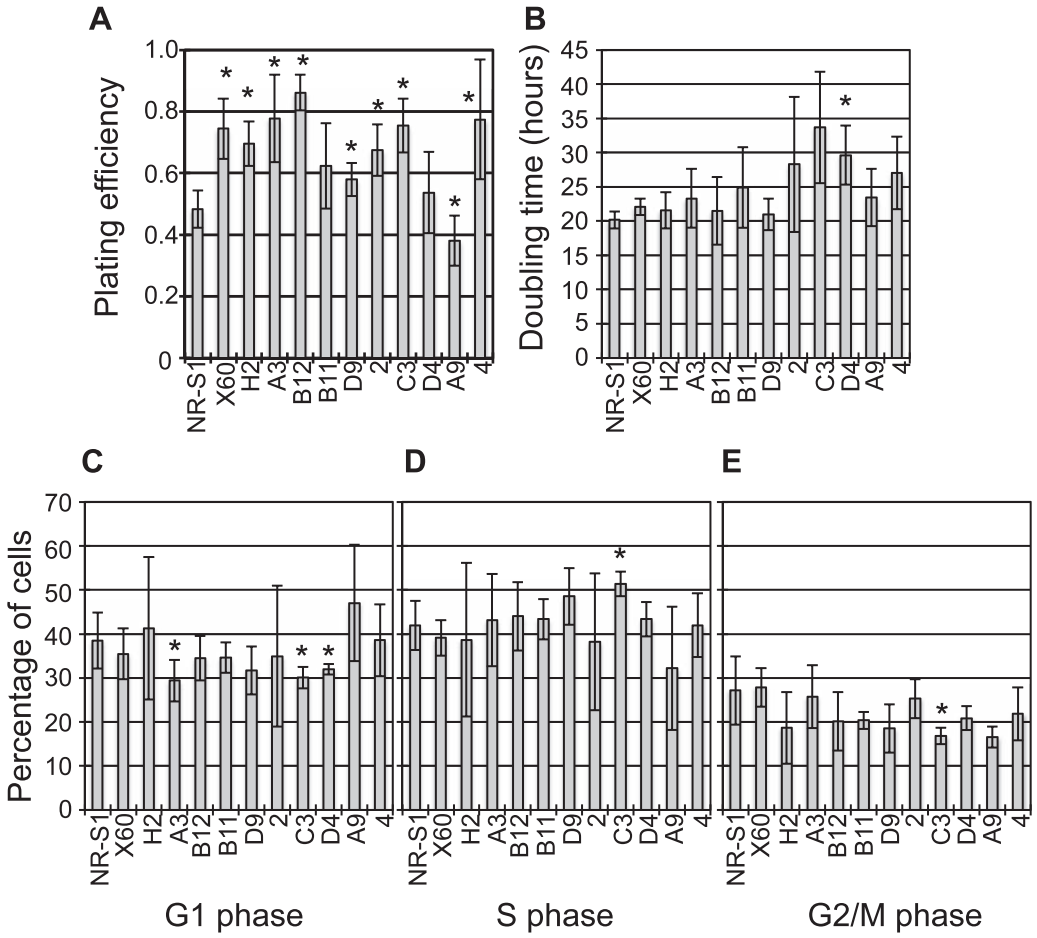


FIG. 5. Difference in cellular property between NR-S1, X60 cells and the subclones. Panels A–E show the plating efficiency (panel A), doubling time (panel B) and percentages of cell cycle distribution (panels C–E). The values and error bars indicate the mean value and standard deviation, respectively, from 3 independent experiments. Asterisks represent a significant difference of $P < 0.05$ using the t test.

contrast, the G_1 phase in X60-A3, X60-C3 and X60-D4 cells decreased to 29.4%, 30.1% and 32.0%, respectively (Fig. 5C), and S phase in X60-C3 cells increased to 51.3%. (Fig. 5D). The percentage of G_2/M phase in X60-C3 cells increased to 62.0% (Fig. 5E).

These results demonstrated that increase in radioresistance might be associated with some morphological end points. If these end points were significantly correlated with each other, it is possible that this approach could be used as a novel marker for radiation-induced radioresistance in cancer cells. Therefore, we statistically analyzed the correlation between the radiosensitivity and the morphological features (Supplementary Fig. S4; http://dx.doi.org/10.1667/RR13492.1.S1). There was good correlation between X-ray resistance and carbon-ion resistance [($R = 0.87$, $P = 0.00053$) Fig. 6A and B; Supplementary Fig. S4], and the heterochromatin domain number was strongly correlated with X-ray resistance ($R = 0.74$, $P = 0.0098$) and carbon-ion resistance ($R = 0.79$, $P = 0.0038$) (Fig. 6A–C; Supplementary Fig. S4). Additionally, the elongation index was correlated with carbon-ion resistance [($R = 0.75$, $P = 0.0085$) Supplementary Fig. S4] but not with X-ray resistance. Futhermore, there was a significant inverse correlation detected between percentage of S phase and that of G_1 phase [($R = -0.82$, $P = 0.0018$) Supplementary Fig. S4]. Other factors, such as cellular size, DNA contents, plating efficiency and doubling time were not significantly correlated with X-ray and C-ion resistance.

These results indicate that repeated exposure to X rays can induce various phenotypic changes in irradiated NR-S1 cells. In particular, the increase in heterochromatin domain number is significantly correlated with X-ray and carbon-ion resistance. These results suggest that the enhancement of heterochromatin formation might be associated with induced X-ray and C-ion resistance.

Disappearance of γ-H2AX Foci in Radioresistant Cell and Parental Cell

Recently, heterochromatin has attracted attention as a platform for DNA repair. We hypothesized that the observed increase in heterochromatin domain number may be associated with enhancement of DNA repair ability in

Downloaded From: https://bioone.org/journals/Radiation-Research on 29 Mar 2024
Terms of Use: https://bioone.org/terms-of-use

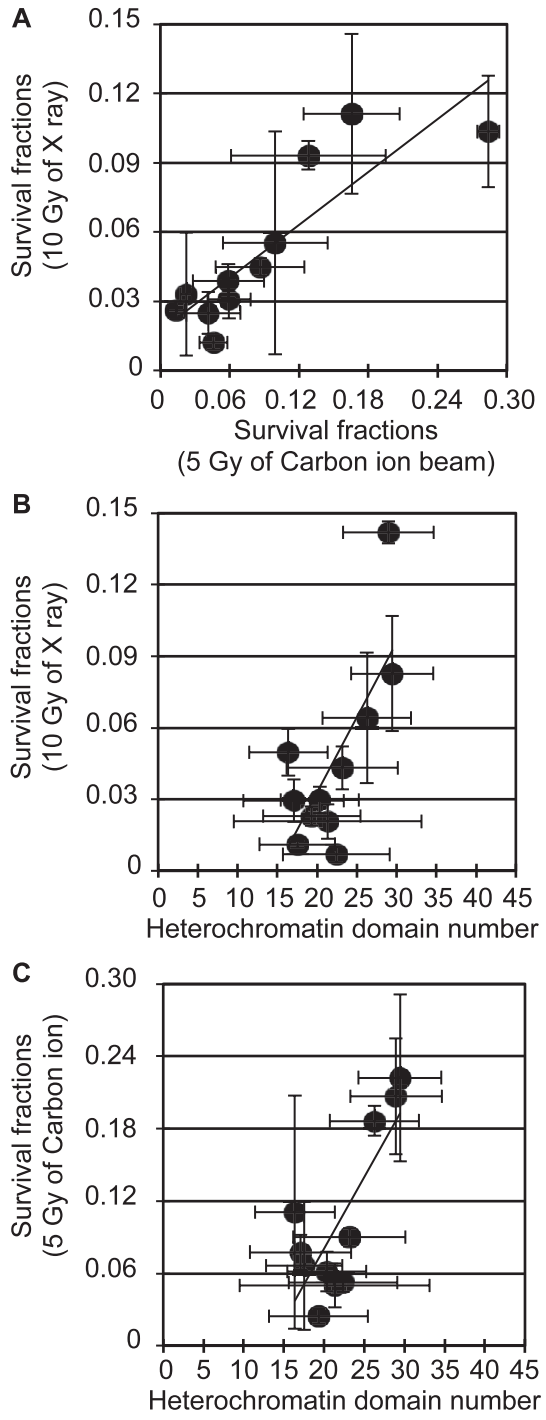


FIG. 6. The correlation between X-ray and carbon-ion resistance and heterochromatin domain number. The statistical difference of these proportions is shown in Supplementary Fig. S4. Panel A shows the correlation between X-ray and carbon-ion sensitivity. Panel B shows the correlation between X-ray sensitivity and heterochromatin domain number. Panel C shows the correlation between carbon-ion sensitivity and heterochromatin domain number. The values and error bars indicate the mean and the standard deviation, respectively, from 3–5 independent experiments with 3 replicates per experiments.

radioresistant cells. To investigate whether DNA repair is promoted in X-ray and C-ion resistant X60 cells and their radioresistant subclones, X60-A3 and X60-H2, we evaluated for the induction and the disappearance of γ-H2AX foci after 10 Gy of X-rays or 5 Gy of carbon-ion irradiation. In X60, X60-A3 and X60-H2 cells, 24 h after X-ray or C-ion irradiation γ-H2AX foci had almost completely disappeared and the remaining number of foci was extremely low compared with that in NR-S1 cells (Fig. 7). For X rays, the mean value of γ-H2AX foci at 24 h postirradiation in X60, X60-A3 and X60-H2 cells was 2.5-, 1.4- and 1.7-fold lower, respectively, than that in NR-S1 cells. Similarly, the number of γ-H2AX foci after carbon-ion irradiation was decreased by 2.5-, 1.4- and 1.7-fold in respective cell lines (Fig. 8).

To confirm whether the DNA repair potential is promoted in X60, X60-H2 and X60-A3 cells, the initial number of γ-H2AX foci must be assessed. After 30 min of exposure to 10 Gy and 5 Gy of X ray and carbon ion, respectively, γ-H2AX foci overlapped each other and therefore could not be accurately counted (Fig. 7). Alternatively, we counted the initial number of γ-H2AX foci per unit dose (Supplementary Fig. S5A and B; http://dx.doi.org/10.1667/RR13492.1.S1) because it is well known that the γ-H2AX foci number is proportional to radiation dose (*17*). When the cells were 1 Gy X irradiated, the number of γ-H2AX foci in the X60 and X60-H2 cells was approximately the same as in the NR-S1 cells. On the other hand, the γ-H2AX foci number in X60-A3 cells was 1.3-fold higher than that in NR-S1 cells. When the cells were C-ion irradiated, there was no difference in the γ-H2AX foci number between X60, X60-H2 and X60-A3 cells.

As expected, these results demonstrated that DNA double-strand break (DSB) repair ability, which was measured by the disappearance of γ-H2AX foci, was significantly enhanced in both X-ray and C-ion resistant cancer cells.

DISCUSSION

Induced Carbon-Ion Resistance by Repetitive Exposure to X Rays

Our study demonstrated that repeated exposure to X rays generated not only X-ray radioresistance but also C-ion radioresistance in irradiated cancer cells. Although the development of X-ray resistance in cancer cells after repeated exposure to X rays has been previously reported (*10–14*), the cells studied in those reports were not evaluated for sensitivity to particle ion beams such as carbon ions.

In addition, our results show that subclone cells (X60-D4, X60-A9 and X60-4) have C-ion resistance but not X-ray resistance. While this appears to contradict the general consensus that C-ion irradiation is more effective for treating X-ray resistant tumors (*8, 9*), X60 cells and their

Downloaded From: https://bioone.org/journals/Radiation-Research on 29 Mar 2024
Terms of Use: https://bioone.org/terms-of-use

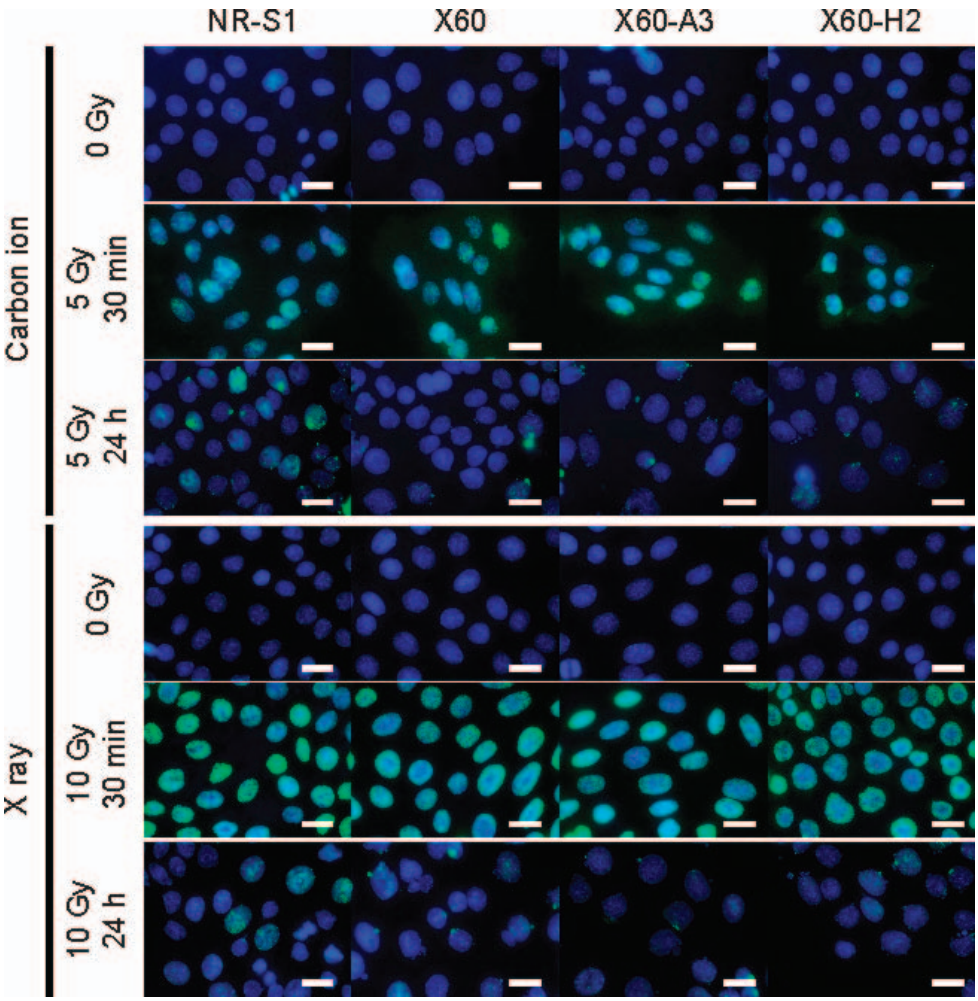


FIG. 7. γ-H2AX foci at indicated times after X-ray or carbon-ion irradiation. The nucleus was stained with 10 μ*M* of Hoechst 33342. The nucleus and γ-H2AX are shown in blue and green, respectively. The scale bars indicate 25 μm.

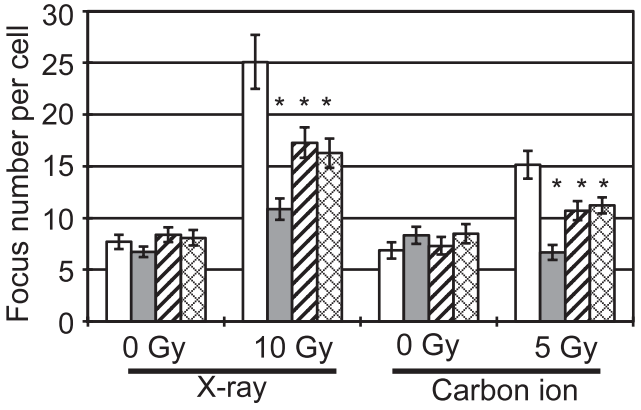


FIG. 8. γ-H2AX foci numbers among radioresistant cell lines are compared. White, gray, slashed and meshed boxes indicate the foci numbers of NR-S1, X60, X60-A3 and X60-H2, respectively. The boxes and error bars indicate the mean and the standard error, respectively. At least 120 cells were counted for calculating the mean value and standard error. The reproducibility of data was confirmed in 3 independent experiments. Asterisks represent a significant difference of $P < 0.05$ using the t test.

subclones could be used as novel experimental models for investigating C-ion resistance in cancer cells. The reason that C-ion resistance was generated in the X60, X60-H2, X60-A3 and X60-B12 cells by repeated exposure to X rays might be a result of cross-resistance between X rays and C-ion irradiation. In many studies, radiation is given as fractions of 0.5–2 Gy (*10–14*), and the radiation is repeated to a total dose of approximately 60 Gy (*10–13*). In our study, the development of C-ion radioresistance in X-ray irradiated cells might be due to the comparatively high dose (fractions size of 10 Gy) we used for X-ray irradiation. At this dose range, complex damage generally associated with heavy-ion radiation may increase even in X-ray irradiated cells. Assuming that the DNA damage induced by high-dose X-ray irradiation is similar to that by C-ion irradiation and that the cancer cell is therefore able to develop radioresistance to both types of radiation, the development of C-ion resistance in X60 cells could be explained by an induction of cross-resistance. However, our results also showed that some subclones, especially X60-D4, X60-A9

Downloaded From: https://bioone.org/journals/Radiation-Research on 29 Mar 2024
Terms of Use: https://bioone.org/terms-of-use

and X60-4 cells, developed C-ion resistance but not X-ray resistance. Although the reason for this is unclear, it may have been caused by differences in the type of enhanced DNA repair in the cells that developed resistance to both radiation types versus the cells specifically that became resistant to carbon ions only. For example, complex DNA damage may contain a crosslink product such as DNA-protein crosslink (DPC) (*18, 19*). If such a product is yielded by repeated exposure to high-dose X rays and the removal capacity of DPC, which is associated with nucleotide excision repair and homologous recombination repair (*20*), is selectively enhanced in X60-D4, X60-A9 and X60-4 cells, these cells might develop resistance only to C-ion radiation. This possibility is based on a previous report that the DPC is effectively induced by high-LET irradiation compared with low-LET irradiation (*21*). Although the precise mechanisms of DPC repair in mammalian cells are largely unknown and further assessment is needed to prove the DPC repair in radioresistant cells since the hypothesis remains speculative, X60 and each of the subclones are nevertheless useful for analyzing the difference between induced X-ray and C-ion resistance in cancer cells.

Relationship between Heterochromatin Formation and X-Ray and C-Ion Resistance

In addition to demonstrating the development of C-ion resistance in X60 cells, we showed that X-ray and C-ion resistance is significantly correlated with the heterochromatin domain number. Since the relationship between C-ion resistance and heterochromatin formation has never been previously reported, these novel results may prove valuable in further investigations of the relationship between radioresistance and chromatin structure.

Some studies have shown that the DNA repair in heterochromatin is different from that in euchromatin (*22–28*). Goodarzi *et al*. found that the DSB repair in heterochromatin requires chromatin relaxation by ataxia telangiectasia mutated (ATM) dependent phosphorylation of Krüppel-associated box (KRAB) domain-associated protein 1 (KAP-1), and that the heterochromatic DSB is repaired at a later time after DSB induction compared with euchromatin. (*22*). This ''slow'' component of DSB repair is conducted not only when DNA damage occurs in the heterochromatin but also at any complex DSB sites induced by high-LET radiation such as carbon ions (*26*). Moreover, the slow component of DSB repair is preferentially performed in the G_2 phase rather than the G_1 phase by homologous recombination (*26, 27*). Shibata *et al*. have proposed a mechanism of DSB repair that starts with nonhomologous end joining (NHEJ) first attempting to repair the heterochromatic DNA damage and this NHEJ repair represents the ''fast'' component of DNA repair, and the remaining DSBs are then repaired by homologous recombination, which is the slow component of DNA repair (*26*). In addition, Chiolo *et al*. found that the DSB repair in heterochromatin was mainly dependent on the homologous recombination pathway and required cell cycle checkpoint proteins such as ATM and ATR. Their study also showed that the heterochromatin region, which contains the HP1α protein, is expanded approximately 30 min after X irradiation, and the DSB site is then relocalized outside of the heterochromatin and then repaired by Rad51 in the late step of homologous recombination (*28*). While their study was performed using *Drosophila* cells, similar results were demonstrated with mouse embryonic fibroblast cells (*29*). Jakob *et al*. revealed that accumulation of γ-H2AX and XRCC1 foci at heterochromatic DSB sites occurred immediately after heavy-ion irradiation, and that these foci were moved from the center to the periphery of heterochromatin domains within approximately 20 min. They also showed that ATM is required for DSB repair in the periphery of heterochromatin domains. While the NHEJ has been shown to modify broken DNA ends through the endonuclease activity of Artemis, homologous recombination repair resects the broken DNA end and then newly synthesizes DNA using the information obtained from sister chromatids in S and G_2 phases. Therefore, homologous recombination repair can more precisely restore the broken DNA DSBs compared with NHEJ repair even though the damaged DNA end structure is more complex (*30*). Since in our study we found the X60 cells were more resistant to the C-ion irradiation and have many heterochromatin domains, the DSB repair component in heterochromatin may likely contribute to the C-ion resistance in X60 cells. These possibilities are emphasized by the cell cycle analysis (Fig. 5C–E, Supplementary Figs. S6 and S7; http://dx.doi.org/10.1667/RR13492.1.S1). While the results showed that the cell cycle distributions in nonirradiated conditions for all cells were approximately the same (Fig. 5C–E), the percentages in G_1 and S phase in X60, X60-A3 and X60-H2 cells after 6 Gy X irradiation were lower and higher, respectively, than those in NR-S1 cells, although these data were not statistically significant (Supplementary Figs. S6 and S7). These results suggest that the contribution of homologous recombination in X60, X60-H2 and X60-A3 cells may be relatively higher than in NR-S1 cells. In addition, heterochromatin components such as heterochromatin protein 1 (HP1) and chromatin assembly factor-1 (CAF-1) are known to promote homologous recombination repair. HP1 and CAF1 have been shown to accumulate in the heterochromatin and the localization of these proteins is changed depending on the chromatin organization (*31–33*). Taken together, these reports suggest that the expression and localization of heterochromatin components such as HP1 in X60 cells possibly differ from those in NR-S1 cells. In fact, the immunofluorescence staining of HP1β clearly showed that the maximum intensity of HP1β fluorescent signal in X60 cells was approximately twofold greater than that in NR-S1 cells (Supplementary Fig. S2E and F; http://dx.doi.org/10.1667/RR13492.1.S1), although further investigation is necessary to confirm the protein expression and

Downloaded From: https://bioone.org/journals/Radiation-Research on 29 Mar 2024
Terms of Use: https://bioone.org/terms-of-use

localization of heterochromatin components. Other laboratories have reported that γ-H2AX focus formation after X irradiation is enhanced by disruption of chromatin structure due to inhibition of histone deacetylase activity (*34*) and the chromatin condensation itself confers the radioresistance compared with decondensed chromatin (*35*). While we must further investigate whether the expression of heterochromatin components and chromatin structure in X60 cells affect X-ray and/or C-ion resistance, these reports support the hypothesis that the enhancement of heterochromatin formation contributes to X-ray and C-ion resistance by promoting DNA repair ability.

An additional question that remains is why the heterochromatin domain number was increased in X60 cells. One of the reasons might just be selection of cells with higher DNA contents and polyploidy. If the polyploid cells were condensed by repeated exposure to X rays, the result will be an increased pericentromeric heterochromatin number in the irradiated cells. To satisfy this condition, the polyploid cells must be radioresistant. However, some studies have shown that the ploidy and DNA contents did not correlate with the radiosensitivity (*36, 37*), and our data agreed with these results (Supplementary Fig. S4; http://dx.doi.org/10.1667/RR13492.1.S1). In addition, we have shown here that the heterochromatin domain number did not significantly correlate with DNA contents (Supplementary Fig. S4). This means that the selection of cells with higher ploidy or DNA contents by repeated exposure to X rays does not sufficiently explain the increased heterochromatin domain number in X60 cells and radioresistant subclones. Another explaination for the increased heterochromatin domain number might be associated with constitution and function of heterochromatin. In general, repeated DNA sequences, such as ribosomal DNA, satellite DNA and transposable elements are enriched in the heterochromatin region (*38*). These DNA sequences may threaten genomic integrity when DNA repair, replication and recombination of these sequences cannot be properly performed (*38, 39*). Although the precise role of heterochromatin formation or chromatin condensation in the maintenance of repeated DNA sequences is currently unclear, the heterochromatin formation may maintain genome integrity, protecting against irregular insertions, recombinations and abnormal expansions of repeated DNA sequences (*40*). Moreover, evidence that the heterochromatin formation contributes to the maintenance of genomic stability has been suggested by some other studies (*41, 42*). Zhu *et al*. have reported that BRCA1, a component of homologous recombination repair and a tumor suppressor, is essential for heterochromatin formation and for the transcriptional repression of tandemly repeated satellite DNA (*41*). In addition, they showed that the ectopic expression of satellite DNA transcripts induced abnormal mitosis and DNA damage. In another study, it was reported that loss of suppressor of variegation 3–9 homolog 1 (SUV39H1), which is a marker of constitutive heterochromatin and a histone methyltransferase that trimethylates lysine 9 on histone H3, led to genomic instability (*42*). Given these data, it is possible that the promoted heterochromatin formation in X60 cells and radioresistant subclones protects the genomic integrity against the abnormal expansion of repeated DNA sequence. These would suggest that heterochromatin formation is necessary for the maintenance of genomic integrity, and our results may support that the promotion of heterochromatin formation may be necessary for the radioresistance acquisition after repeated exposure to X rays.

SUPPLEMENTARY INFORMATION

Fig. S1. Irradiation procedure for establishment of resistant cancer cells.

Fig. S2. Colocalization of Hoechst 33342 intense foci and HP1β foci in NR-S1 (panels A and B) and in X60 cells (panels C and D). The HP1β foci were visualized by means of immunofluorescence staining, described in the Materials and Methods section, using anti-HP1β antibody (Cell Signaling Technology Inc., Danvers, MA). The nucleus was stained with 10 μ*M* of Hoechst 33342. The HP1β and Hoechst 33342 foci are shown in red and blue, respectively. Panels B and D are magnified images of the regions marked by a white square shown in panels A and C, respectively. The fluorescence image of each cell was acquired under the same optical configuration. The fluorescence intensity profiles of NR-S1 (panel E) and X60 cells (panel F) were measured along the white line shown in panels B and D, respectively. The red and blue lines represent the intensity profiles of HP1β and Hoechst 33342, respectively. The scale bars indicate 25 μm for panels A and C, and 10 μm for panels B and D. These results showed that the HP1β focus, which is marker of constitutive heterochromatin, was well colocalized with the Hoechst 33342 intense focus.

Fig. S3. Hoechst 33342 and HP1β colocalization in selected subclones. The HP1β and Hoechst 33342 are shown in red and blue, respectively. The scale bars indicate 25 μm.

Fig. S4. Summary of the correlation coefficients. The pairwise comparison of Pearson's product-moment correlation coefficient was calculated. The color scale under the correlation matrix indicates the strength of the correlation coefficient. When the *P* value is less than 0.05, the correlation coefficient is regarded as statistically different and is underlined.

Fig. S5. Initial number of γ-H2AX foci. After 30 min of 1 Gy X or carbon-ion irradiation, the cells were fixed with 10% buffered formalin. Then γ-H2AX foci were visualized by the methods described in the Methods and Materials section. Panel A shows the γ-H2AX foci formation in NR-S1, X60, X60-A3 and X60-H2 cells. The nucleus and γ-H2AX are shown in blue and green. The scale bars indicate 25 μm. Panel B shows the γ-H2AX foci number indicated in panel A. White, gray, slashed and meshed boxes,

Downloaded From: https://bioone.org/journals/Radiation-Research on 29 Mar 2024
Terms of Use: https://bioone.org/terms-of-use

respectively indicate the foci number of NR-S1, X60, X60-A3 and X60-H2 cells. The boxes and error bars indicate the mean value and standard error. At least 100 cells were counted for calculating the mean value and standard error. The reproducibility of data was confirmed in three independent experiments. Asterisks represent a significant difference of $P < 0.05$ using the t test.

Fig. S6. Cell cycle progression after 6 Gy X irradiation. The cells were fixed at indicated time point after X irradiation.

Fig. S7. Percentages in each phase shown in Supplementary Fig. S6.

ACKNOWLEDGMENTS

This work was supported by JPSP KAKENHI grant numbers 25861141, 24591857 and 24249067 and was a research project with heavy ions at NIRS-HIMAC.

Received: July 30, 2013; accepted: June 14, 2014; published online: September 17, 2014

REFERENCES

1. Onishi H, Araki T, Shirato H, Nagata Y, Hiraoka M, Gomi K, et al. Stereotactic hypofractionated high-dose irradiation for stage I non small cell lung carcinoma: clinical outcomes in 245 subjects in a Japanese multiinstitutional study. Cancer 2004; 101:1623–31.
2. Onishi H, Shirato H, Nagata Y, Hiraoka M, Fujino M, Gomi K, et al. Hypofractionated stereotactic radiotherapy (HypoFXSRT) for stage I non-small cell lung cancer: updated results of 257 patients in a Japanese multi-institutional study. J Thorac Oncol 2007; 2 Suppl 3:S94–100.
3. Combs SE, Kalbe A, Nikoghosyan A, Ackermann B, Jakel O, Haberer T, et al. Carbon ion radiotherapy performed as re-irradiation using active beam delivery in patients with tumors of the brain, skull base and sacral region. Radiother Oncol 2011; 98:63–7.
4. Belli M, Bettega D, Calzolari P, Cherubini R, Cuttone G, Durante M, et al. Effectiveness of monoenergetic and spread-out bragg peak carbon-ions for inactivation of various normal and tumour human cell lines. J Radiat Res 2008; 49:597–607.
5. Tinganelli W, Ma NY, Von Neubeck C, Maier A, Schicker C, Kraft-Weyrather W, et al. Influence of acute hypoxia and radiation quality on cell survival. J Radiat Res 2013; 54:i23–30.
6. Hirayama R, Uzawa A, Takase N, Matsumoto Y, Noguchi M, Koda K, et al. Evaluation of SCCVII tumor cell survival in clamped and non-clamped solid tumors exposed to carbon-ion beams in comparison to X-rays. Mutat Res 2013; 756:146–51.
7. Hall EJ, Giaccia AJ. Radiobiology for the radiologist. 7th ed. Philadelphia: Lippincott Williams & Wilkins: 2012, p. 104–13.
8. Yanagi T, Mizoe JE, Hasegawa A, Takagi R, Bessho H, Onda T, et al. Mucosal malignant melanoma of the head and neck treated by carbon ion radiotherapy. Int J Radiat Oncol Biol Phys 2009; 74:15–20.
9. Kamada T, Tsujii H, Tsuji H, Yanagi T, Mizoe JE, Miyamoto T, et al. Efficacy and safety of carbon ion radiotherapy in bone and soft tissue sarcomas. J Clin Oncol 2002; 20:4466–71.
10. Shimura T, Kakuda S, Ochiai Y, Nakagawa H, Kuwahara Y, Takai Y, et al. Acquired radioresistance of human tumor cells by DNA-PK/AKT/GSK3β-mediated cyclin D1 overexpression. Oncogene 2010; 29:4826–37.
11. Russell J, Wheldon TE, Stanton P. A radioresistant variant derived from a human neuroblastoma cell line is less prone to radiation-induced apoptosis. Cancer Res 1995; 55:4915–21.
12. Lynam-Lennon N, Reynolds JV, Pidgeon GP, Lysaght J, Marignol L, Maher SG. Alterations in DNA repair efficiency are involved in the radioresistance of esophageal adenocarcinoma. Radiat Res 2010; 174:703–11.
13. Pearce AG, Segura TM, Rintala AC, Rintala-Maki ND, Lee H. The generation and characterization of a radiation-resistant model system to study radioresistance in human breast cancer cells. Radiat Res 2001; 156:739–50.
14. Kuwahara Y, Li L, Baba T, Nakagawa H, Shimura T, Yamamoto Y, et al. Clinically relevant radioresistant cells efficiently repair DNA double-strand breaks induced by X-rays. Cancer Sci 2009; 100:747–52.
15. Tamaki T, Iwakawa M, Ohno T, Imadome K, Nakawatari M, Sakai M, et al. Application of carbon-ion beams or gamma-rays on primary tumors does not change the expression profiles of metastatic tumors in an in vivo murine model. Int J Radiat Oncol Biol Phys 2009; 74:210–8.
16. Schaffner B, Kanai T, Futami Y, Shimbo M, Urakabe E. Ridge filter design and optimization for the broad-beam three-dimensional irradiation system for heavy-ion radiotherapy. Med Phys 2000; 27:716–24.
17. Sedelnikova OA, Rogakou EP, Panyutin IG, Bonner WM. Quantitative detection of ^{125}IdU-induced DNA double-strand breaks with gamma-H2AX antibody. Radiat Res 2002; 158:486–92.
18. Shoulkamy MI, Nakano T, Ohshima M, Hirayama R, Uzawa A, Furusawa Y, et al. Detection of DNA-protein crosslinks (DPCs) by novel direct fluorescence labeling methods: distinct stabilities of aldehyde and radiation-induced DPCs. Nucleic Acids Res 2012; 40:e143.
19. Barker S, Weinfeld M, Murray D. DNA-protein crosslinks: their induction, repair, and biological consequences. Mutat Res 2005; 589:111–35.
20. Ide H, Shoulkamy MI, Nakano T, Miyamoto-Matsubara M, Salem AM. Repair and biochemical effects of DNA-protein crosslinks. Mutat Res 2011; 711:113–22.
21. Culard F, Bouffard S, Charlier M. High-LET irradiation of a DNA-binding protein: protein-protein and DNA-protein crosslinks. Radiat Res 2005; 164:774–80.
22. Goodarzi AA, Jeggo P, Lobrich M. The influence of heterochromatin on DNA double strand break repair: getting the strong, silent type to relax. DNA Repair (Amst) 2010; 9:1273–82.
23. Goodarzi AA, Jeggo PA. The heterochromatic barrier to DNA double strand break repair: how to get the entry visa. Int J Mol Sci 2012; 13:11844–60.
24. Murray JM, Stiff T, Jeggo PA. DNA double-strand break repair within heterochromatic regions. Biochem Soc Trans 2012; 40:173–8.
25. Goodarzi AA, Noon AT, Deckbar D, Ziv Y, Shiloh Y, Lobrich M, et al. ATM signaling facilitates repair of DNA double-strand breaks associated with heterochromatin. Mol Cell 2008; 31:167–77.
26. Shibata A, Conrad S, Birraux J, Geuting V, Barton O, Ismail A, et al. Factors determining DNA double-strand break repair pathway choice in G2 phase. EMBO J 2011; 30:1079–92.
27. Beucher A, Birraux J, Tchouandong L, Barton O, Shibata A, Conrad S, et al. ATM and Artemis promote homologous recombination of radiation-induced DNA double-strand breaks in G2. EMBO J 2009; 28:3413–27.
28. Chiolo I, Minoda A, Colmenares SU, Polyzos A, Costes SV, Karpen GH. Double-strand breaks in heterochromatin move outside of a dynamic HP1a domain to complete recombinational repair. Cell 2011; 144:732–44.
29. Jakob B, Splinter J, Conrad S, Voss KO, Zink D, Durante M, et al. DNA double-strand breaks in heterochromatin elicit fast repair protein recruitment, histone H2AX phosphorylation and relocation to euchromatin. Nucleic Acid Res 2011; 39:6489–99.
30. Durante M, Bedford JS, Chen DJ, Conrad S, Cornforth MN, Natarajan AT, et al. From DNA damage to chromosome aberrations: joining the break. Mutat Res 2013; 756:5–13.

Downloaded From: https://bioone.org/journals/Radiation-Research on 29 Mar 2024
Terms of Use: https://bioone.org/terms-of-use

31. Luijsterburg MS, Dinant C, Lans H, Stap J, Wiernasz E, Lagerwerf S, et al. Heterochromatin protein 1 is recruited to various types of DNA damage. J Cell Biol 2009; 185:577–86.

32. Baldeyron C, Soria G, Roche D, Cook AJ, Almouzni G. HP1alpha recruitment to DNA damage by p150CAF-1 promotes homologous recombination repair. J Cell Biol 2011; 193:81–95.

33. Houlard M, Berlivet S, Probst AV, Quivy JP, Hery P, Almouzni G, et al. CAF-1 is essential for heterochromatin organization in pluripotent embryonic cells. PLoS Genet 2006; 2:e181.

34. Zhang Y, Adachi M, Zou H, Hareyama M, Imai K, Shinomura Y. Histone deacetylase inhibitors enhance phosphorylation of histone H2AX after ionizing radiation. Int J Radiat Oncol Biol Phys 2006; 65:859–66.

35. Takata H, Hanafusa T, Mori T, Shimura M, Iida Y, Ishikawa K, et al. Chromatin compaction protects genomic DNA from radiation damage. PLoS One 2013; 8:e75622.

36. Schwartz JL. The radiosensitivity of the chromosomes of the cells of human squamous cell carcinoma cell lines. Radiat Res 1992; 129:96–101.

37. Mariya Y, Streffer C, Fuhrmann C, Wojcik A. Correlation of radiation-induced micronucleus frequency with clonogenic survival in cells of one diploid and two tetraploid murine tumor cell lines of the same origin. Radiat Res 1997; 147:29–34.

38. Peng JC, Karpen GH. Epigenetic regulation of heterochromatic DNA stability. Curr Opin Genet Dev 2008; 18:204–11.

39. Slotkin RK, Martienssen R. Transposable elements and the epigenetic regulation of the genome. Nat Rev Genet 2007; 8:272–85.

40. Pearson CE, Nichol Edamura K, Cleary JD. Repeat instability: mechanisms of dynamic mutations. Nat Rev Genet 2008; 6:729–42.

41. Zhu Q, Pao GM, Huynh AM, Suh H, Tonnu N, Nederlof PM, et al. BRCA1 tumour suppression occurs via heterochromatin-mediated silencing. Nature 2011; 477:179–84.

42. Peters AH, O' Carroll D, Scherthan H, Mechtler K, Sauer S, Schofer C, et al. Loss of the Suv39h histone methyltransferases impairs mammalian heterochromatin and genome stability. Cell 2001; 107:323–37.

Downloaded From: https://bioone.org/journals/Radiation-Research on 29 Mar 2024
Terms of Use: https://bioone.org/terms-of-use